ISSN 0020-4412, Instruments and Experimental Techniques, 2017, Vol. 60, No. 3, pp. 428–433. © Pleiades Publishing, Ltd., 2017.
Original Russian Text © S.V. Rogozhkin, A.A. Aleev, A.A. Lukyanchuk, A.S. Shutov, O.A. Raznitsyn, S.E. Kirillov, 2017, published in Pribory i Tekhnika Eksperimenta, 2017, No. 3, pp. 129–134.

LABORATORY TECHNIQUES

# An Atom Probe Tomography Prototype with Laser Evaporation

**S. V. Rogozhkin[a,b]*, A. A. Aleev[a,b], A. A. Lukyanchuk[a,b], A. S. Shutov[a,b], O. A. Raznitsyn[a,b], and S. E. Kirillov [b]**

[a] *Institute for Theoretical and Experimental Physics named by A.I. Alikhanov of National Research Centre "Kurchatov Institute", Moscow, 117218 Russia*

[b] *National Research Nuclear University MEPhI (Moscow Engineering Physics Institute), Moscow, 115409 Russia*

**e-mail: sergey.rogozhkin@itep.ru; SVRogozhkin@mephi.ru*

Received April 29, 2016; in final form, July 13, 2016

**Abstract**—The results of development, creation, and tests of an atom-probe prototype with femtosecond laser evaporation and a position-sensitive microchannel detector with delay lines for the tomographic (3D) analysis of chemical composition of materials are presented. The atom-probe tomography is based on the principle of atom-by-atom "disassembling" of materials and projection magnification, which was previously used in field-ion microscopy, as well as the time-of-flight mass spectrometry that is applied to each evaporated ion. The prototype characteristics (mass resolution, spatial resolution, and data-collection efficiency) were demonstrated in study of tungsten.

**DOI:** 10.1134/S002044121702021X

## INTRODUCTION

The atom-probe tomography (APT) makes it possible to perform a detailed chemical analysis of materials with a virtually atomic spatial resolution. The high spatial resolution of the APT is based on the same projection principle as that in the field-ion microscopy (FIM), which was developed by Muller in the 1950s [1, 2]. The applied potential difference between the sample–needle and a detector provides the motion of ions along definite trajectories, thus allowing one to unambiguously relate the coordinates of the arrival of the atom at a position-sensitive detector to the coordinates of its removal from the sample. At the same time, the applied potential difference is always below the threshold of the field ion evaporation from the sample surface. The evaporation of ions from the sample surface results from an additional pulsed action that allows registration of the time of the ion escape from the sample and determination of the time of flight of an evaporated ion after it hits the detector. As a result, the data are used to determine the mass-to-charge ratio for the particle that was evaporated from the sample and the particle position on the sample. A working prototype of a tomographic atom probe, a so-called PoSAP, was presented in 1980 [3]. Subsequently, various concepts of APT facilities were proposed and tested [4–6].

Because the APT technique allows one to conduct investigations of materials with nanostructural specific features, this technique is especially in demand in modern materials science. In particular, APT investigations make it possible to reveal nanosize precipitations that contain only several atoms and ascertain the chemical nature of each of them [7–10]. By analyzing the samples that were subjected to various thermal and radiation actions using an atom probe, one can observe the growth or dissolving dynamics of nanoprecipitations, changes in their composition and distribution of elements, the evolution of the local chemical composition and the cluster structure, etc. [10]. Investigations of the above phenomena using an atom probe have unique capabilities that exceed those of other techniques up to now [9, 11]. In Russia, APT investigations began in 2003 at the Institute of Theoretical and Experimental Physics [12] on the ECOTAP (CAMECA) energy-compensated optical tomographic atom probe. A considerable part of these studies was devoted to investigations of the nanostructures of reactor materials both in the initial state [7, 8] and after the irradiation with neutrons [9, 10] or ions [11, 13]. In all the above cases, the APT investigations made it possible to reveal the specific features of the chemical composition of the nanostructures of steels, which are unattainable with other techniques.

A specific feature of the ECOTAP is the electric-pulse evaporation of atoms from a sample, which

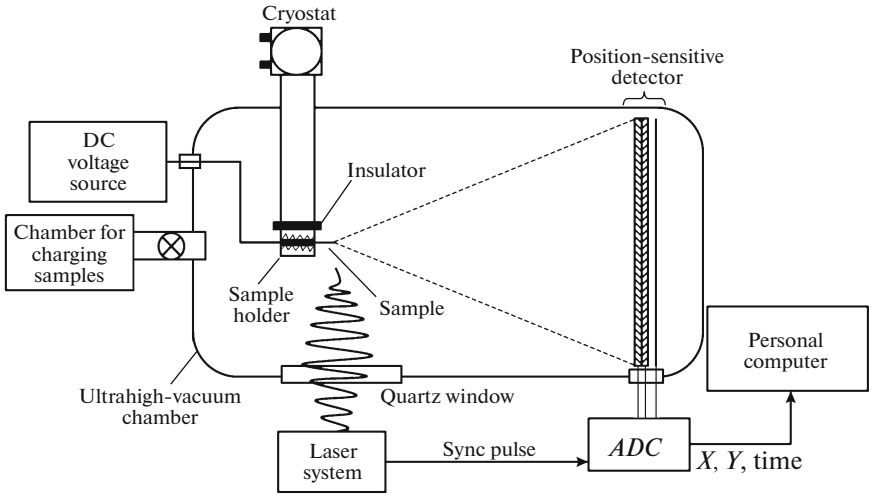


**Fig. 1.** A diagram of the APPLE-3D atom-probe prototype with laser evaporation and a detector on delay lines. *ADC* is the analog-to-digital converter.

allows to investigate conducting materials. The application of a reflectron [14] provided a rather high mass resolution: $M/\Delta M \geq 600$. The investigated volumes were on average ~10 × 10 × (100–500) nm$^3$. The value of the cross section of the investigated volume is determined mainly (at a fixed geometry) by the size of the detector (~80 mm), while the depth of the investigated volume is determined by the stability of a particular sample under the influence of the evaporating action, which enhances with an increase in the radius of the sample tip during the experiment. The data collection rate (1–10 atoms/s) is limited by the speed of operation of the optical camera that is used in the ECOTAP detector to determine the position of an ion that arrives.

The APT technique has been actively developed in the recent years. New types of detecting and evaporating systems were introduced and the data-reconstruction algorithms were improved [15]. This paper presents the results of the development of an atom probe prototype (APPLE-3D) with the use of a position-sensitive microchannel detector with delay lines (DLD detector) and laser evaporation of atoms for the tomographic analysis of the chemical composition of materials.

## EXPERIMENTAL SETUP SCHEME

As mentioned above, the APT technique involves the controlled evaporation of atoms from the sample surface and their subsequent detection [3]. In the developed prototype, controlled evaporation is performed using a pulse laser source. The use of a laser makes it possible to investigate a wide range of materials: metals, semiconductors, ceramics, glasses, and even some biological objects [16–18]. A position-sensitive DLD detector that allows an increase in the data-collection rate by more than one order of magnitude in comparison with the ECOTAP facility was chosen as the detection system. It also provides the detection of multiple events (simultaneous arrival of several particles at the detector). The simplest geometry, in which the sample–needle is placed opposite the detector, is used in the APPLE-3D (see Fig. 1). The distance from the sample tip to the detector is ~183 mm. This geometry makes it possible to avoid difficulties in the adjustment of additional ion-deflecting systems [18, 19] and also allows the application of standard data-reconstruction algorithms [20].

## THE VACUUM SYSTEM

When atom-probe investigations are conducted, it is necessary to provide an ultrahigh vacuum in the analyzed volume. The diagram of the arrangement of the vacuum volumes is shown in Fig. 2. CF-type compounds with copper spacers were used. The vacuum volumes are evacuated using two- or three-stage systems of pumps (Pfeiffer Vacuum) for the charging and analytical volumes. The first stage for both volumes is a dry scroll backing pump; it provides a rarefaction of ~$10^{-3}$ Torr. Further, turbomolecular pumps are installed: one on the charging chamber and two on the analytical volume. The pressures in the chambers are measured with hot-cathode ionization vacuum gauges. The pressures in the analytical and charging volumes are $5.0 \times 10^{-10}$ and $4.0 \times 10^{-9}$ Torr, respectively.

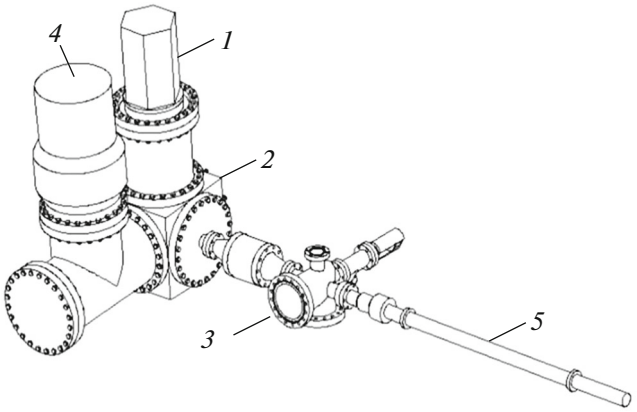


**Fig. 2.** The diagram of the arrangement of the main vacuum volumes of the APPLE-3D: (*1*) cryosystem; (*2*) measurement volume; (*3*) air-lock chamber; (*4*) turbomolecular pump; and (*5*) transfer rod.

## APT SAMPLES AND THEIR LOADING INTO THE APPLE-3D

The investigated samples–needles are prepared of metal strips with dimensions of 0.3 × 0.3 × (10–15) mm, one of whose ends is treated using the electrochemical technique in order to obtain the tip radius about 50–100 nm. In this case, it is necessary that the sample tapering be no larger than 11°. The sample shape is controlled using a transmission electron microscope (an example of the sample image is shown in Fig. 3a). The other end of the metal wire is tightly fixed first in a nickel tube and then in a copper tube, which is finally inserted into a special copper chuck. Figure 3b shows the elements of the sample holder. When the sample is charged into the prototype, the chuck with the sample is attached to a rod through the charging chamber; after the charging chamber is evacuated, the chuck is transferred to the analytical volume, where it is fixed in the holder to be investigated. The same rod is used to extract the sample after the investigation.

Since a high voltage is fed to the sample, the chuck must be electrically insulated from other units of the system. For this purpose, the outer part of the holder of the chuck with the sample (which is fixed in the working volume) is manufactured of ceramics. This holder is also attached to a system of cryoconductors that lead to a PT805 cryohead (produced by Cryo-Mech). This cryosystem allows a sample to be cooled to 20 K. The majority of APT investigations are performed within a temperature range of 20–80 K.

## THE DETECTION SYSTEM

A position-sensitive detector on the basis of Roent-Dek DLD120 delay lines with an effective diameter of 120 mm is used to detect evaporated ions. The detecting system consists of an assembly of microchannel plates (MCPs) and a system of anodes, an amplifier of a signal from the detector, and an analog-to-digital converter (ADC) for digitizing and transmitting data to the computer. Data can be digitized at a sampling frequency of up to 5 GHz. The detection principle is based on the delay lines [21]. An ion enters a channel of the MCP and generates a cloud of electrons, which then arrive at the system of anodes. The signal is then amplified in the amplification module and transmitted to the ADC. The coordinates of particles that hit the detector are determined with an accuracy of better than 100 μm, thus making it possible to provide a spatial resolution of the prototype that approaches the atomic resolution. The size of the detector substantially exceeds that of the detectors in modern industrially produced LEAP 3000 or LEAP 4000 apparatuses. The effective area of the detector together with a 183-mm ion flight length allow one to attain a data-collection angle of ≈32°, which is comparable to that in analogous facilities [22].

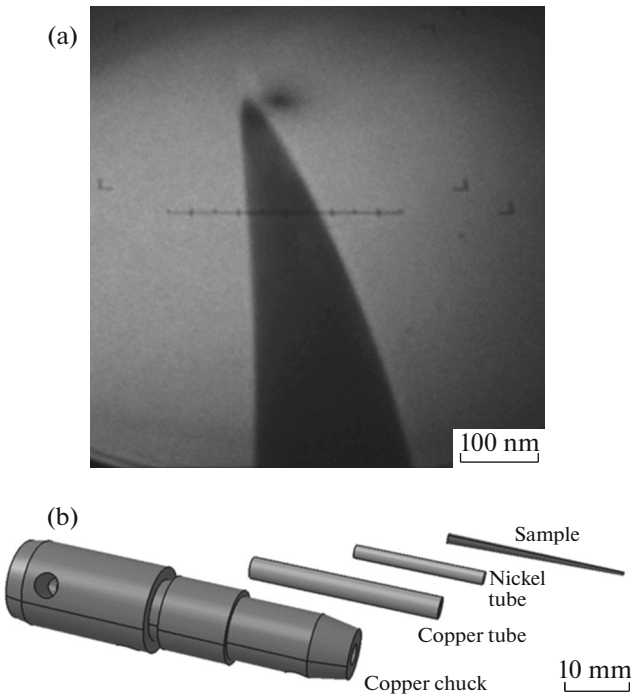


**Fig. 3.** (a) An example of the image of the tip of a ready sample in the transmission electron microscope and (b) elements of the sample holder.

## THE EVAPORATION SYSTEM

DC voltage from a FuG Electronik GmbH high-voltage source (up to 13 kV) is fed to a sample to evaporate atoms (ions). A TEAT-25ST laser system (produced by Avesta-Proekt, Moscow) is used as the pulse-evaporation source. This system allows generation of pulses with a duration of 60 fs. The pulse energy

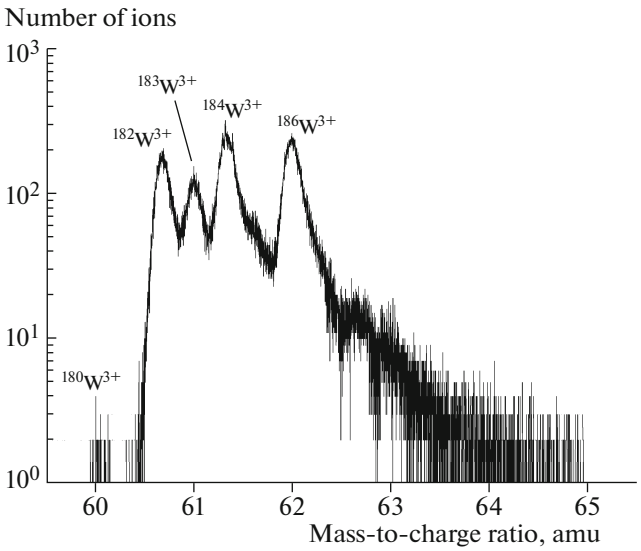


**Fig. 4.** A mass spectrum that was obtained using the APPLE-3D in studies of a tungsten sample.

ranges from 0.1 to 250 μJ and is chosen before the experiment depending on the sample material. The fundamental wavelength is 1030 nm, which allows three harmonics for evaporating a sample to be obtained: 515, 343, and 257 nm. These wavelengths make it possible to investigate metals and semiconductors [23], as well as some dielectrics [24]. The operating laser frequency is at most 50 kHz. Laser radiation is focused using a system of lenses to the tip of the sample; the diameter of the laser beam on the sample is ~50 μm. The laser beam is injected into the investigation chamber using a system of mirrors and stepping motors, which provide a positioning accuracy of better than 2 μm. The laser beam is injected into the vacuum volume through a special quartz window with a transmittance of greater than 95% for each of the above three harmonics. The laser system also generates a sync pulse for measuring the time of flight of particles, which is then fed to the input of the ADC module in the detection system.

## APT INVESTIGATION TECHNIQUE

After a sample is loaded into the analytical volume and the slide gate, which separates air-lock and measurement volumes, is closed, the vacuum in the latter volume is reduced to values of ~$5.0 \times 10^{-10}$ Torr and the sample is cooled to temperatures of 20–80 K to minimize the thermal motion of atoms. Subsequently, a constant positive voltage is fed to the sample to create a field at the sample that is required for the evaporation (approximately 10 V/nm) [25]. Because the radius of the sample tip is small, the required evaporation-inducing field can be attained by applying only several kilovolts. It should be noted that the produced field is close to the spontaneous evaporation of the material but insufficient for its onset. To initiate the evaporation, the sample is irradiated with a laser pulse. The selected laser-radiation intensity is such that the probability of evaporating one ion from the sample within one pulse is ~0.05 [26]. The evaporated ion escapes from the sample surface perpendicular to it along the field lines. Because the field near the sample tip is inversely proportional to the distance to its surface, its accelerating effect rapidly becomes weak and the ion flies further at a fixed velocity and virtually rectilinearly. The detector fixes the moment of the arrival of the ion; as a result, the time of the ion flight that passed from the instant of its evaporation from the sample surface due to the pulse action is determined. The coordinates of the point of the ion arrival at the detector are also registered. All of the data from the detection and evaporation systems is then entered to the computer. The evaporation procedure of material atoms is repeated many times until the sample degrades or the study is stopped by an operator. The file of collected data includes the consecutively written data on each registered ion: the coordinates of its arrival at the detector, its time of flight, and the evaporation voltage. After the data are collected, the mass spectrum can be identified and the 3D arrangement of ions can be reconstructed using a special data-reconstruction program [26].

## THE CHARACTERISTICS OF THE APPLE-3D DEVICE

The operability of the prototype was tested using polycrystalline tungsten. This metal evaporates rather well, has a high melting temperature, and has a body-centered cubic crystallographic lattice with a lattice parameter of 0.316 nm. Figure 4 shows the measured mass spectrum in which the peaks of all stable tungsten isotopes, which correspond to ions with a charge of $3^+$, are clearly observed. Tungsten ions with other charges were not detected. The mass resolution $M/\Delta M$ was greater than 600 at the peak half-height of the $^{184}W$ tungsten isotope.

Figure 5 shows the atomic map of the investigated volume of the sample, on which each point corresponds to a detected tungsten ion. Atoms of other types were not detected. To determine the egress locations of crystallographic planes on the surface of the investigated sample–needle, a 2D histogram of the distribution of events on the detector was constructed (Fig. 6).

The types of crystallographic directions were determined according to this diagram. The atomic planes in the (100) direction, which is virtually coaxial to the investigated sample, can be also observed in the atomic map (Fig. 5) of the sample. It is known that the best spatial APT resolution is attained precisely in the

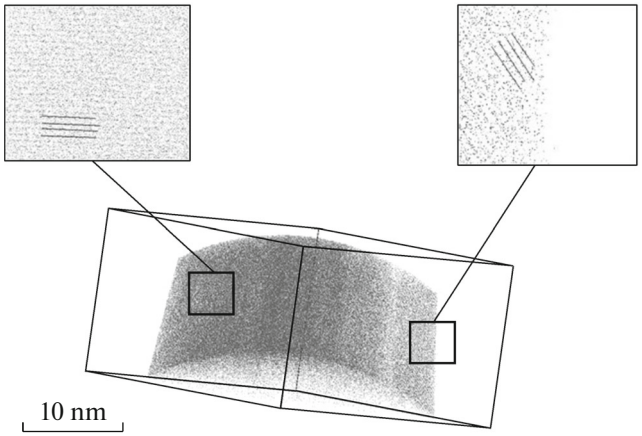


**Fig. 5.** The atomic map of a part of the investigated volume of the tungsten sample. The enlarged fragments show the atomic planes that correspond to two different egress points of the crystallographic planes.

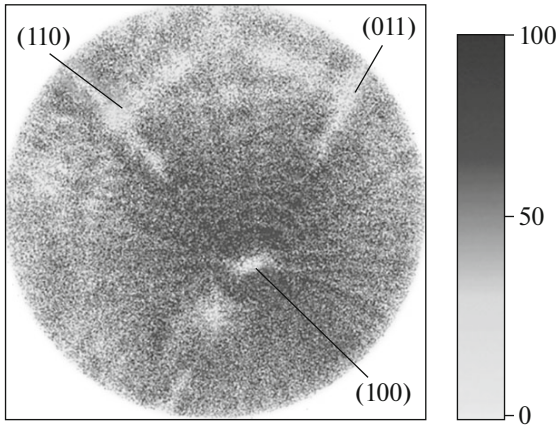


**Fig. 6.** A 2D histogram of the events distribution on the detector: (dark gray) the maximum and (white) minimum number of events.

direction of the sample axis [22]. The measured interplanar distance is 1.58 ± 0.03 Å, which coincides with the tabulated value (1.58 Å) within the error limit. Atomic planes in the (011) direction, which lie at an angle to the sample axis, are also seen in the atomic map (Fig. 5). The measured interplanar distance for these planes is 1.9 ± 0.3 Å, which coincides with the tabulated value (2.23 Å) within the error limit. Observing these planes from two different crystallographic egress locations allows one to consider that the lateral resolution of the APPLE-3D is ~2–4 Å and the depth resolution is ~1–2 Å. Note that the obtained spatial resolution is characteristic of most APT facilities.

## CONCLUSIONS

The APPLE-3D atom-probe prototype with laser evaporation and a detector on delay lines, which was developed and put into operation at the Institute for Theoretical and Experimental Physics named by A.I. Alikhanov of National Research Centre "Kurchatov Institute", is described. The results of the study of tungsten samples on the APPLE-3D facility showed that the investigated area is ~50 × 50 × 1000 nm$^3$, the mass resolution is more than 600, and the spatial resolution is no worse than 4 Å. The facility performs efficient investigations of virtually any metal sample and has potential for studying semiconductors and dielectrics.

## REFERENCES

1. Müller, E.W., Panitz, J.A., and McLane, S.B., *Rev. Sci. Instrum.,* 1968, vol. 39, no. 1, p. 83.
2. Müller, E.W., *Z. Physik*, 1951, vol. 131, no. 1, p. 136. doi 10.1007/BF01329651
3. Kellogg, G. and Tsong, T., *J. Appl. Phys.,* 1980, vol. 51, no. 2, p. 1184.
4. Miller, M.K., Cerezo, A., Hetherington, M.G., and Smith G.D.W., *Atom Probe Field Ion Microscopy,* London: Oxford Sci. Publ., 1996.
5. Miller, M.K., *Atom Probe Tomography,* New York: Kluwer Academic, 2000.
6. *High Resolution Imaging and Spectrometry of Materials,* Al-Kassab, T., Wollenberger, H., Schmitz, G., Kirchheim, R., Ernst T., and Ruhle, M., Eds., Berlin: Springer-Verlag, 2003.
7. Rogozhkin, S.V., Ageev, V.S., Aleev, A.A., Zaluzhnyi, A.G., Leont'eva-Smirnova, M.V., and Nikitin, A.A., *Phys. Met. Metallogr.,* 2009, vol. 108, no. 6, p. 579. doi 10.1134/S0031918X09120084
8. Aleev, A.A., Iskandarov, N.A., Klimenkov, M., Lindau, R., Möslang, A., Nikitin, A.A., Rogozhkin, S. V., Vladimirov, P., and Zaluzhnyi, A.G., *J. Nuclear Materials,* 2011, vol. 409, no. 2, p. 65. doi 10.1016/j.jnucmat.2010.09.008
9. Rogozhkin, S.V., Aleev, A.A., Zaluzhnyi, A.G., Nikitin, A.A., Iskandarov, N.A., Vladimirov, P., Lindau, R., and Möslang, A., *J. Nuclear Materials,* 2011, vol. 409, no. 2, p. 94. doi 10.1016/j.jnucmat.2010.09.021
10. Kryukov, A., Debarberis, L., Ballesteros, A., Krsjak, V., Burcl, R., Rogozhkin, S. V., Nikitin, A.A., Aleev, A.A., Zaluzhnyi, A.G., Grafutin, V.I., Ilyukhina, O., Funtikov, Yu.V., and Zeman, A., *J. Nuclear Materials,* 2012, vol. 429, nos. 1–3, p. 190. doi 10.1016/ j.jnucmat.2012.06.005
11. Rogozhkin, S.V., Aleev, A.A., Zaluzhnyi, A.G., Kuibida, R.P., Kulevoi, T.V., Nikitin, A.A., Orlov, N.N., Chalykh, B.B., and Shishmarev, V.B., *Phys. Met. Metallogr.,* 2012, vol. 113, no. 2, p. 200. doi 10.1134/S0031918X12020111
12. Suvorov, A.L., Rogozhkin, S.V., Zaluzhnyi, A.G., Aleev, A.A., Bobkov, A.F., Zaitsev, S.V., Karpov, A.V., Kozodaev, M.A., Loginov, B.A., and Makeev, O.N., *Vopr. At. Nauki Tekhn. Ser.: Materialoved. Nov. Mater.,* 2006, no. 1, p. 3.

13. Rogozhkin, S.V., Orlov, N.N., Aleev, A.A., Zaluzhnyi, A.G., Kozodaev, M.A., Kuibeda, R.P., Kulevoy, T.V., Nikitin, A.A., Chalykh, B.B., Lindau, R., Möslang, A., and Vladimirov, P., *Phys. Met. Metallogr.,* 2015, vol. 116, no. 1, p. 72. doi 10.1134/S0031918X150100939

14. Cerezo, A., Godfrey, T.J., Sijbrandij, S.J., Smith, G.D.W., and Warren, P.J., *Rev. Sci. Instrum.*, 1998, vol. 69, no. 1, p. 49. doi 10.1063/1.1148477

15. Bas, P., Bostel, A., Deconihout, B., and Blavette, D., *Appl. Surf. Sci.,* 1995, vol. 87/88, p. 298. doi 10.1016/0169-4332(94)00561-3

16. Silaeva, E.P., Shcheblanov, N.S., Itina, T.E., Vella, A., Houard, J., Sévelin-Radiguet, N., Vurpillot, F., and Deconihout, B., *Appl. Phys. A: Mater. Sci. Proces.,* 2013, vol. 110, no. 3, p. 703. doi 10.1007/s00339-012-7189-7

17. Oberdorfer, C. and Schmitz, G., *Microsc. Microanal.,* 2011, vol. 17, no. 1, p. 15. doi 10.1017/S1431927610093888

18. Gordon, L.M. and Joester, D., *Nature,* 2011, vol. 469, no. 7329, p. 194. doi 10.1038/nature09686

19. Cerezo, A., Godfrey, T.J., Sijbrandij, S.J., Smith, G.D.W., and Warren, P.J., *Rev. Sci. Instrum.,* 1998, vol. 69, no. 1, p. 49. doi 10.1063/1.1148477

20. Bemont, E., Bostel, A., Bouet, M., da Costa, G., Chambreland, S., Deconihout, B., and Hono, K., *Ultramicroscopy,* 2003, vol. 95, nos. 1–4, p. 231. doi 10.1016/S0304-3991(02)00321-2

21. Jagutzki, O., Cerezo, A., Czasch, A., Dorner, R., Hattass, M., Huang, M., Mergel, V., Spillmann, U., Ullmann-Pfleger, K., Weber, T., Schmidt-Bocking, H., and Smith, G.D.W., *IEEE Trans. Nucl. Sci.,* 2002, vol. 49, no. 5, p. 2477. doi 10.1109/TNS.2002.803889

22. Stender, P., Oberdorfer, C., Artmeier, M., Pelka, P., Spaleck, F., and Schmitz, G., *Ultramicroscopy,* 2007, vol. 107, no. 9, p. 726. doi 10.1016/j.ultramic.2007.02.032

23. Inoue, K., Yano, F., Nishida, A., Takamizawa, H., Tsunomura, T., Nagai, Y., and Hasegawa, M., *Ultramicroscopy,* 2009, vol. 109, no. 12, p. 1479. doi 10.1016/j.ultramic.2009.08.002

24. Gault, B., Menand, A., de Geuser, F., Deconihout, B., and Danoix, R., *Appl. Phys. Lett.,* 2006, vol. 88, no. 11, p. 14101. doi 10.1063/1.2186394

25. Sakurai, T. and Müller, E.W., *Phys. Rev. Lett.,* 1973, vol. 30, no. 12, p. 532. doi 10.1103/PhysRevLett.30.532

26. Miller, M.K. and Forbes, R.G., *Atom-Probe Tomography. The Local Electrode Atom Probe,* London: Springer-Verlag, 2014. doi 10.1007/978-1-4899-7430-310

*Translated by A. Seferov*